Raman scattering intensities of layered crystals

S. Nakashima
Laboratoire de Physique des Solides, Université Pierre et Marie Curie, 4 place Jussieu, 75230 Paris Cédex 05, France and Department of Applied Physics, Faculty of Engineering, Osaka University, Yamadaoka, Suita, Osaka 565 Japan

M. Balkanski
Laboratoire de Physique des Solides, Université Pierre et Marie Curie, 4 place Jussieu, 75230 Paris Cédex 05, France
(Received 19 March 1986)

Raman polarizability tensors for layered crystals, CdI_2, GaSe, and red HgI_2 are calculated on the basis of the bond-polarizability concept. It is shown that out-of-plane folded modes are missing or very weak. Missing modes arise from the cancellation of the bond Raman polarizabilities within a unit cell. From a comparison with observed Raman spectra the nature of the atomic bonding is discussed.

I. INTRODUCTION

Since the discovery of Raman effect, Raman spectroscopy has been well established. However, there still remain essential problems which are unresolved. One of the problems is the explanation of one-phonon Raman scattering intensities of solids. The analysis of the Raman intensity has been made mainly for molecules[1-3] and second-order phonons in IV-IV and III-V compound semiconductors.[4-6] Raman polarizability tensors have been so far calculated for one-phonon modes in cubic crystals.[7,8] Lopez-Cruz and Cardona have attempted to interpret the Raman spectrum of the $4H$ modification of Ge using their calculated Raman tensors.[9] However, very little work has been reported on the Raman intensity profiles of one-phonon modes in solids which show relatively complex spectra.

In order to interpret relative Raman intensities we have developed a model based on the bond polarizability concept.[10,11] This model has explained qualitatively the relative Raman intensity of the zone-folded modes of various CdI_2 polytypes.[12] More recently, this model has been applied to SiC polytypes and the calculated Raman polarizability tensors of folded modes showed a qualitative agreement with the observation.[13] This model is based on the concept that the vibrational modes are coherent waves and the compensation in contributions from the Raman polarizability tensors of respective bonds (or interatomic Raman polarizability) occurs partially or almost completely, depending on crystal structure and atomic displacement pattern. The satisfying results in the interpretation of Raman intensity profiles of folded modes suggest that the model is applicable to the Raman intensity of phonon modes which lie originally at the Γ point in the basic polytype, and also to phonon modes in crystals showing no polytypes.

In this work we have calculated the Raman polarizability tensors for three typical layered crystals, CdI_2, GaSe, and red HgI_2, and compared them with the experimental results. The calculated results predict that certain phonon modes are missing or very weak. A comparison with experimental results provides information about the bonding nature of the crystals.

II. CALCULATION OF THE RAMAN POLARIZABILITY TENSORS

The first derivatives of the electronic polarizability tensors, i.e., Raman polarizability tensors are derived using the concept of the bond polarizability.[1,4,13] In this derivation electronic polarizabilities are assumed to be given as a sum of the electronic polarizabilities for bonds between the nearest-neighbor pair of atoms, each of which depends only on the bond length. Under these assumptions, the tensor components of the polarizability of the unit cell in a crystal are given by

$$\alpha_{\rho\sigma}=\sum_{j=1}^{N_B}[(\alpha_{||}^{j}-\alpha_{\perp}^{j})(j\rho)(j\sigma)+\alpha_{\perp}^{j}\delta_{\rho\sigma}]\ , \tag{1}$$

where $\alpha_{||}$ and $\alpha_{\perp}$ are longitudinal and transverse components of the bond polarizability, respectively. $(j\rho)$ represents the direction cosine of the jth bond with the ρth crystal axis, and N_B is the number of chemical bonds.

The net polarizability given by Eq. (1) depends on bond lengths and bond orientations. Raman polarizability tensor for the λth mode is expressed as a first derivative of the electronic polarizability with respect to the normal coordinate Q_λ,

$$\alpha'_{\rho\sigma}(\lambda)=\frac{\partial\alpha_{\rho\sigma}}{\partial Q_\lambda}\ , \tag{2}$$

where the derivative is evaluated at the equilibrium positions.

We express this quantity by using so-called intensity coordinates[1] whose elements consist of bond stretching Δr_n and changes of direction cosines $\Delta(nX)$ and $\Delta(nY)$, because Eq. (1) is not expressed explicitly as a function of the normal coordinates. Intensity coordinates are related to Cartesian displacement coordinates by the matrix $\underline{T}$. Thus we may write

$$\underline{I}=\underline{T}\,\underline{X}\ . \tag{3}$$

The relation between the $3m$ Cartesian displacement coordinates and the normal coordinates Q may be written as

$$\underline{Q}=\underline{A}\,\underline{M}^2\,\underline{X}=\underline{R}\,\underline{U}\ , \tag{4}$$

where $\underline{M}=[(M_i)^{1/2}\delta_{ij}]$, m is the number of atoms in a unit cell and M_i is the mass of the ith atom and we put $\underline{M}\,\underline{X}=\underline{R}\,\underline{U}$. The matrix $\underline{A}$ is constructed from the eigenvectors of the equation of motion,

$$\sum_j(\delta_{ij}M_j\omega^2-D_{ij})A_j=0\ , \tag{5}$$

where D_{ij} is the force constant matrix.

Using Eqs. (4) and (5) and the relations $\underline{A}=\underline{R}\,\underline{M}^{-1}$ and $\underline{R}^{-1}=\underline{\tilde{R}}$, we get the following relation:

$$\underline{I}=\underline{T}\,\underline{\tilde{A}}\,\underline{Q}\ , \tag{6}$$

where the tilde denotes the transpose of a matrix. Combining Eqs. (2) and (6), we have

$$\underline{\left[\frac{\partial\alpha_{\rho\sigma}}{\partial Q_\lambda}\right]}=\underline{\left[\frac{\partial\alpha_{\rho\sigma}}{\partial I_r}\right]}\underline{T}\,\underline{\tilde{A}}\ , \tag{7}$$

where I_r is the rth element of the intensity coordinates. We may write the row matrix $\underline{(\partial\alpha_{\rho\sigma}/\partial I_r)}$ as a sum of the derivative of the individual bond polarizability $[\alpha_n]$,

$$\frac{\partial\alpha\rho\sigma}{\partial Ir}=\sum_n^{N_B}\left[\cdots,\frac{\partial[\alpha_n]_{\rho\sigma}}{\partial r_n},\frac{\partial[\alpha_n]_{\rho\sigma}}{\partial(nX)},\frac{\partial[\alpha_n]_{\rho\sigma}}{\partial(nY)},\cdots\right]. \tag{8}$$

Using this equation, we have

$$\begin{aligned}\frac{\partial\alpha_{\rho\sigma}}{\partial Q_\lambda}=\sum_{n=1}^{N_B}\Bigg[&\frac{\partial[\alpha_n]_{\rho\sigma}}{\partial x_i}(A_{\lambda x_i}-A_{\lambda x_p})\\&+\frac{\partial[\alpha_n]_{\rho\sigma}}{\partial y_i}(A_{\lambda y_i}-A_{\lambda y_p})\\&+\frac{\partial[\alpha_n]_{\rho\sigma}}{\partial z_i}(A_{\lambda z_i}-A_{\lambda z_p})\Bigg]\ ,\end{aligned} \tag{9}$$

where displacement amplitudes $A_{\lambda r_i}$ and $A_{\lambda r_p}$ are not zero only if two atoms whose positions are given by r_i and r_p are the end atoms of the nth bond, and

$$\begin{aligned}\frac{\partial[\alpha_n]_{\rho\sigma}}{\partial x_i}=&\frac{\partial[\alpha_n]_{\rho\sigma}}{\partial r_n}\frac{\partial r_n}{\partial x_i}\\&+\frac{\partial[\alpha_n]_{\rho\sigma}}{\partial(nx)}\frac{\partial(nX)}{\partial x_i}+\frac{\partial[\alpha_n]_{\rho\sigma}}{\partial(nY)}\frac{\partial(nY)}{\partial x_i}\ .\end{aligned} \tag{10}$$

The phonons at the Γ point in layered crystals are divided into in-plane modes (shear-type modes), and out-of-plane modes (compression-type modes) for which atoms in an atomic plane perpendicular to the c axis move as a whole. Since all the atoms in an atomic plane are equivalent for these modes, Eq. (9) may be written as

$$\frac{\partial\alpha_{\rho\sigma}}{\partial Q_\lambda}=\sum_s\alpha_{\rho\sigma,x}(s)[A_{\lambda x}(s)-A_{\lambda x}(s+1)]\ , \tag{11}$$

for x polarization, where $A_{\lambda x}(s)$ is the displacement amplitude of sth atomic plane and the sum over s is taken over a unit cell. The quantity $\alpha_{\rho\sigma,x}(s)$ in Eq. (11) is expressed as

$$\alpha_{\rho\sigma,x}(s)=\sum_m\frac{\partial[\alpha_m]_{\rho\sigma}}{\partial x_i}\ . \tag{12}$$

In Eq. (12) the sum over m is taken over all the bonds between s and $(s+1)$th atomic planes. The equations similar to Eq. (11) hold for y and z polarizations. The Raman polarizability for a bond, i.e., the bond Raman polarizability is easily calculated if the crystal structure is given. The matrix $\underline{T}$ consists of 3×3 submatrices. The submatrix related to the nth bond is expressed as

$$\underline{T}_s=\begin{array}{c}\begin{matrix}(nX)&(nY)&(nZ)\end{matrix}\\\begin{bmatrix}\frac{1}{r}[1-(nX)^2] & \frac{1}{r}(nX)(nY) & \frac{1}{r}(nX)(nZ)\\ \frac{1}{r}(nX)(nY) & \frac{1}{r}[1-(nY)^2] & \frac{1}{r}(nY)(nZ)\end{bmatrix}\end{array}\ , \tag{13}$$

where r is the bond length.

So far the bond polarizability model has been applied only to strongly covalent crystals. However, this model is applicable to partially ionic crystals as well as van der Waals crystals,[12] in which nonbonded valence electrons contribute much to Raman polarizabilities. Our calculated tensor forms reflect correctly crystal symmetry. The method developed in this paper will be widely used to obtain Raman tensors for other crystals if one takes into account appropriately the effect of nonbonded electrons on the Raman tensor components.

III. RAMAN POLARIZABILITY TENSORS IN LAYERED CRYSTAL

A. CdI_2 family

A various number of polytypes have been found in CdI_2. We assume in the calculation that the structures of an I-Cd-I layer of CdI_2 polytypes are the same as that of the ideal CdI_2 ($c/a=1.633$). For CdI_2 polytypes, it is sufficient to consider the two groups of bonds (i) $A\beta C$, $B\gamma A$, and $C\alpha B$, and (ii) $A\gamma B$, $B\alpha C$, and $C\beta A$, where Roman and Greek letters denote the positions of anions and cations within a plane perpendicular to the c axis in the hexagonal packing, respectively.[12] Each bond structure of a group gives the same Raman tensor.

The normal coordinates for the in-plane (E-type) and out-of-plane (A-type) modes of the $2H$ polytype which contains one layer in the unit cell are given by[14]

$$S_x=\frac{1}{\sqrt{2}}(x_1-x_3),\quad S_y=\frac{1}{\sqrt{2}}(y_1-y_3)\ , \tag{14}$$

for the E_g mode and

$$S_z=\frac{1}{\sqrt{2}}(z_1-z_3)\ , \tag{15}$$

for the A_g mode, where x_1 and x_3 are the x components of displacements of two iodine planes. The unit cell in the

$2H$ polytype contains six bonds as shown in Fig. 1 and the net Raman tensors for a layer calculated using Eqs. (11), (14), and (15) are given in Table I.

The xx, yy and xy components for the E_g mode have the same magnitude, but are reversed in sign for two groups of bonds (a) and (b), while xz component of the E_g mode and diagonal components of the A_g mode are equal for the two groups. The relative displacement of anions lying in adjacent layers contributes to the Raman tensor of rigid layer (RL) modes in higher polytypes. Since its contribution to the Raman tensors of intralayer modes is considered to be small, we neglect it. We also assume that cations are at rest for Raman active modes in any polytypes (isolated layer approximation). Exactly speaking, bond polarizabilities, their first derivatives and also interatomic forces differ for different layer stackings. However, the difference would be small for the intralayer modes of most layered crystals, because the interlayer forces are quite small compared with intralayer forces and the bonding within a layer is hardly affected by the difference of the stacking. Under these assumptions the components of the Raman polarizability tensor for a layer in Eq. (12), $\alpha_{\rho\sigma,x}(s)$ are independent of s. We obtain the following relation for the A-type modes in polytypes of CdI_2,

$$\frac{\partial\alpha_{\rho\sigma}}{\partial Q_\lambda}=\alpha^{\lambda}_{\rho\sigma}\sum[A_{\lambda z}(s)-A_{\lambda z}(s+1)]\,, \tag{16}$$

where $\alpha^{\lambda}_{\rho\sigma}$ is the component of the Raman polarizability tensor for a layer, and $A_{\lambda z}(s)$ and $A_{\lambda z}(s+1)$ are amplitudes of displacement along the z axis for two iodine-atom planes within a layer.

In Eq. (16) sum is taken over all atomic planes in a unit cell. For the folded modes corresponding to the phonon modes with nonzero wave vector ($q\neq 0$) in the basic zone, there is always a set of relative displacements of anions in the unit cell, which are 180° out of phase with each other. Accordingly, we obtain

$$\sum[A_{\lambda z}(s)-A_{\lambda z}(s+1)]=0\,. \tag{17}$$

This result leads to the conclusion that for any polytypes of the CdI_2 family the folded modes with the A symmetry are missing or their Raman intensities are very weak except for the $q(0)$ mode which lies originally at the Γ point of the basic polytype. The same situation will hold for the folded interlayer modes of A symmetry, i.e., folded modes of the LA branch. In fact the folded modes of the A species are missing in CdI_2 and PbI_2 polytypes.[12,15] Very weak folded modes of the LA branch have been observed in $18R$ SnS_2 only.[16] The relative Raman intensities for folded modes of TA and TO branches in CdI_2 polytypes are analyzed in detail in Ref. 12.

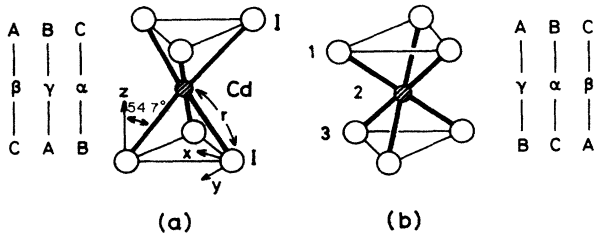

FIG. 1. Structure of $2H$-CdI_2 and bonds in a unit cell for (a) $A\beta C$, $B\gamma A$, and $C\alpha B$ configurations and (b) $A\gamma B$, $B\alpha C$, and $C\beta A$ configurations.

TABLE I. Raman tensors of (a) $A\beta C$, $B\gamma A$, and $C\alpha B$ layers and (b) $A\gamma B$, $B\alpha C$, and $C\beta A$ layers of CdI_2 for the normal modes given in Eqs. (14) and (15). The normalization factors in the normal modes are not included in the Raman tensors. Letters in the parentheses represent the direction of the polarization of phonons. α is the bond polarizability for the Cd—I bond.

	$A_g(z)$	$E_g(x)$	$E_g(y)$
(a)	$\begin{bmatrix} a & 0 & 0 \\ 0 & a & 0 \\ 0 & 0 & b \end{bmatrix}$	$\begin{bmatrix} d & 0 & e \\ 0 & -d & 0 \\ e & 0 & 0 \end{bmatrix}$	$\begin{bmatrix} 0 & -d & 0 \\ -d & 0 & e \\ 0 & e & 0 \end{bmatrix}$
(b)	$\begin{bmatrix} a & 0 & 0 \\ 0 & a & 0 \\ 0 & 0 & b \end{bmatrix}$	$\begin{bmatrix} -d & 0 & e \\ 0 & d & 0 \\ e & 0 & 0 \end{bmatrix}$	$\begin{bmatrix} 0 & d & 0 \\ d & 0 & e \\ 0 & e & 0 \end{bmatrix}$

$$a=\frac{2}{\sqrt{3}}(\alpha'_{\parallel}+2\alpha'_{\perp})-\frac{4}{\sqrt{3}r}(\alpha_{\parallel}-\alpha_{\perp})$$

$$b=\frac{2}{\sqrt{3}}(\alpha'_{\parallel}+2\alpha'_{\perp})+\frac{8}{\sqrt{3}r}(\alpha_{\parallel}-\alpha_{\perp})$$

$$d=\frac{2}{\sqrt{6}}(\alpha'_{\parallel}-\alpha'_{\perp})-\frac{4}{\sqrt{6}r}(\alpha_{\parallel}-\alpha_{\perp})$$

$$e=\frac{2}{\sqrt{3}}(\alpha'_{\parallel}-\alpha'_{\perp})+\frac{2}{\sqrt{3}r}(\alpha_{\parallel}-\alpha_{\perp})$$

B. GaSe family

A GaSe layer contains two types of bonds, Ga—Se and Ga—Ga which is parallel to the c axis. For γ-GaSe, a

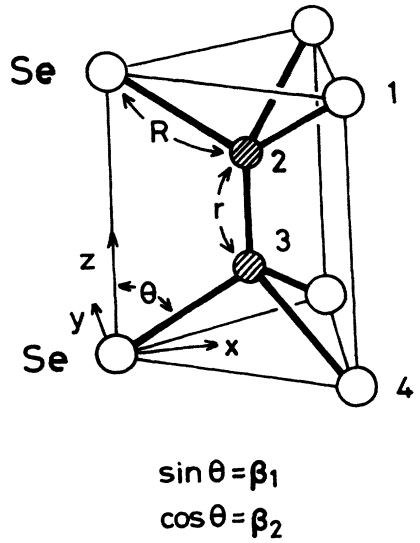

FIG. 2. Structure of γ-GaSe and bonds in a unit cell.

unit cell consists of a layer and seven bonds are included in it as shown in Fig. 2. Raman active modes at the Γ point are represented by[17]

$$\Gamma_{\text{opt}}=3A_1+2E \ .$$

Their normal coordinates are shown in Appendix A. The Raman polarizability tensors calculated for these modes are shown in Table II.

For the A_1^2 mode, Ga—Ga bonds do not vary and the contributions from upper and lower Ga—Se bonds within a layer cancel out. This results in vanishing of all the Raman tensor components, predicting very weak Raman intensity of the A_1^2 mode. As seen in Table II, the polarizability of the Ga—Ga bond contributes to Raman tensors of the A_1^3, A_1^4, E^3, and E^4 modes. As in the case of CdI_2, we assume that the contribution from interlayer bonds is small compared with that of intralayer bonds and that the interlayer bonds contribute only to the RL modes.

The Raman polarizability tensors can be also calculated for ϵ-GaSe for which the unit cell contains two layers and Ga—Se bonds in a layer are rotated by 60° around the c axis with respect to the Ga—Se bonds in counterlayer. For the E-type modes, xz and yz components of the Raman tensors arising from the Ga—Se bonds in layers 1 and 2 have the same magnitude and sign, while other tensor components differ in their sign for these two layers. For the A-type modes, xz and yz components arising from Ga—Se bonds in layer 1 and 2 differ in their sign.

We find that for the ϵ-GaSe polytype Raman tensors arising from intralayer bonds in layer 1 and 2 cancel out for $A_1'^1$ and $A_1'^3$ modes which correspond to the folded modes of A_1^3 and A_1^4 phonon branches of γ-GaSe, respectively, because the atoms in each layer move with 180° out-of-phase. For the same reason, the Raman tensors of the intralayer modes E'^3, E''^1, and E''^3 corresponding to the E^2, E^3, and E^4 modes, respectively, are zero. The calculated Raman tensor for any A_2-type modes in ϵ-GaSe is zero, which is consistent with the fact that the A_2

TABLE II. Raman polarizability tensors for γ-GaSe. Here, β_1 and β_2 are a sine and cosine of the angle between the Ga—Se bond and the c axis, respectively. The bond polarizabilities α with superscript 0 and without superscript are referred to Ga—Ga bond with a length of r and Ga—Se bond with a length of R, respectively. a and b are the coefficients of the displacements described in Appendix A.

E^2 mode

$$\begin{bmatrix} d_2 & 0 & 0 \\ 0 & -d_2 & 0 \\ 0 & 0 & 0 \end{bmatrix}, \quad \begin{bmatrix} 0 & -d_2 & 0 \\ -d_2 & 0 & 0 \\ 0 & 0 & 0 \end{bmatrix}$$

(x) (y)

$$d_2=2(a+b)P_1^{xx}$$

E^3 mode

$$\begin{bmatrix} 0 & 0 & c_2 \\ 0 & 0 & 0 \\ c_2 & 0 & 0 \end{bmatrix}, \quad \begin{bmatrix} 0 & 0 & 0 \\ 0 & 0 & c_2 \\ 0 & c_2 & 0 \end{bmatrix}$$

(x) (y)

$$c_2=2(a-b)P_1^{xz}+2b\frac{1}{r}(\alpha_{||}^0-\alpha_\perp^0)$$

E^4 mode

$$\begin{bmatrix} 0 & 0 & c_2' \\ 0 & 0 & 0 \\ c_2' & 0 & 0 \end{bmatrix}, \quad \begin{bmatrix} 0 & 0 & 0 \\ 0 & 0 & c_2' \\ 0 & c_2' & 0 \end{bmatrix}$$

(x) (y)

$$c_2'=2(a+b)P_1^{xz}-2b\frac{1}{r}(\alpha_{||}^0-\alpha_\perp^0)$$

A_1^2 mode

$$\begin{bmatrix} 0 & 0 & 0 \\ 0 & 0 & 0 \\ 0 & 0 & 0 \end{bmatrix}$$

(z)

A_1^3 mode

$$\begin{bmatrix} a_2 & 0 & 0 \\ 0 & a_2 & 0 \\ 0 & 0 & b_2 \end{bmatrix}$$

(z)

$$a_2=2(a-b)P_3^{xx}+2b\alpha_1^{0\prime}$$

$$b_2=2(a-b)P_3^{zz}+2b\alpha_{||}^{0\prime}$$

A_1^4 mode

$$\begin{bmatrix} a_2' & 0 & 0 \\ 0 & a_2' & 0 \\ 0 & 0 & b_2' \end{bmatrix}$$

(z)

$$a_2'=2(a+b)P_3^{xx}-2b\alpha_1^{0\prime}$$

$$b_2'=2(a+b)P_3^{zz}-2b\alpha_{||}^{0\prime}$$

$$P_1^{xx}=\tfrac{3}{4}(\alpha_{||}'-\alpha_\perp')\beta_1^3-\tfrac{3}{2}\beta_1^3\frac{\alpha_{||}-\alpha_\perp}{R}$$

$$P_1^{xz}=\tfrac{3}{2}(\alpha_{||}'-\alpha_\perp')\beta_1^2\beta_2+\frac{3(\alpha_{||}-\alpha_\perp)}{R}\beta_2^3$$

$$P_3^{xx}=\tfrac{3}{2}(\alpha_{||}'-\alpha_\perp')\beta_1^2\beta_2+3\alpha_\perp'\beta_2-3\beta_1^2\beta_2\frac{(\alpha_{||}-\alpha_\perp)}{R}$$

$$P_3^{zz}=3(\alpha_{||}'-\alpha_\perp')\beta_2^3+3\alpha_\perp'\beta_2+\frac{6\beta_1^2\beta_2}{R}(\alpha_{||}-\alpha_\perp)$$

mode is Raman inactive. The same argument as applied to the CdI_2 family leads to a conclusion that the folded modes with the A symmetry are missing or very weak except for the $q(0)$ mode in GaSe polytypes.

Raman measurements of GaSe have been reported by many researchers.[17] Polarized Raman spectra of γ- and ϵ-GaSe have been measured by Hoff *et al.*[18] Their result has shown that Raman bands at 60, 134, 211, and 309 cm^{-1} are intense, which are assigned to the phonon modes corresponding to E^3, A_1^3, E^4, and A_1^4 modes in γ-GaSe, respectively. The Raman bands of the $A_1'^1$ and A_1^2 types have not yet been observed in ϵ-GaSe. Hoff *et al.*[18] have assigned the Raman band at about 134 cm^{-1} in ϵ-GaSe to $A_1'^2$ mode [$A_1'(1^2)$ by their notation]. This band was tentatively attributed to $A_1'^1$ mode by Wieting and Verble.[17] As mentioned above, the contributions of Raman polarizabilities from respective two layers in the unit cell cancel out for the $A_1'^1$ mode. This suggests that the 134-cm^{-1} band is the $A_1'^2$ mode.

Polian *et al.*[19] have observed a very weak band at 37.2 cm^{-1} in δ-GaSe (four layers per unit cell) whose intensity is about $\frac{1}{60}$ times as weak as that of the E-type rigid layer mode. They have assigned this band to the folded mode of the zone-edge phonon in the A_1' acoustic branch of γ-GaSe. In ϵ-GaSe they have observed a weak Raman band at 56.9 cm^{-1} and ascribed this band to the E''^1 mode which is a Davydov partner of the E''^2 mode at 59.6 cm^{-1}.

The strong Raman intensity of the A_1^3, A_1^4, E^3, and E^4 modes indicates that the contribution of the Ga—Ga bonds to the Raman polarizability is dominant for these modes. This conclusion is consistent with the chemical nature of the Ga—Ga bonds in GaSe. Recent studies on electron distribution in GaSe have demonstrated that the presence of a Ga_2 diatomic molecule is recognized and the electronic charge in the Ga—Ga bond is concentrated between two Ga atomic planes within a layer.[20]

Raman tensor forms for RL modes which arise from interlayer Se—Se bonds are given in Table III. The xx, yy, and xy components for the E-type modes have opposite signs for the interlayer $A-C$ and $C-A$ bonds. Here, following the representation of hexagonal stacking, we shall represent the stacking of ϵ-GaSe as $(A\beta\beta A)(C\alpha\alpha C)$, where Roman and Greek letters refer to Se and Ga atoms, respectively.

TABLE III. The layer Raman tensors for the rigid layer vibrations in GaSe polytypes, which arise from (a) interlayer A(Se)—C(Se) bonds and (b) C(Se)—A(Se) bonds. Only the tensor forms are given for the A- and E type-modes.

	$A(z)$	$E(x)$	$E(y)$
(a)	$\begin{bmatrix} a & 0 & 0 \\ 0 & a & 0 \\ 0 & 0 & a \end{bmatrix}$,	$\begin{bmatrix} d & 0 & e \\ 0 & d & 0 \\ e & 0 & 0 \end{bmatrix}$,	$\begin{bmatrix} 0 & -d & 0 \\ -d & 0 & e \\ 0 & e & 0 \end{bmatrix}$
(b)	$\begin{bmatrix} a & 0 & 0 \\ 0 & a & 0 \\ 0 & 0 & a \end{bmatrix}$,	$\begin{bmatrix} -d & 0 & e \\ 0 & -d & 0 \\ e & 0 & 0 \end{bmatrix}$,	$\begin{bmatrix} 0 & d & 0 \\ d & 0 & e \\ 0 & e & 0 \end{bmatrix}$

For the RL modes of ϵ-GaSe relative displacements of A(Se)-C(Se) and C(Se)-A(Se) planes are out of phase with each other and then the net Raman tensors are given by the difference between the tensors (a) and (b) in this table. It follows that all tensor components are zero for the A-type mode, and xz and yz components are zero for the E-type mode. This result is consistent with the group theoretical prediction that only the E-type RL mode is Raman active for ϵ-GaSe.

C. Red HgI_2

Red HgI_2 belongs to the space group D_{4h}^{15} and the unit cell contains two layers. As shown in Fig. 3, Hg atoms are surrounded tetrahedrally by iodine atoms and eight Hg—I bonds and eight interlayer I—I′ bonds are contained in the unit cell. Raman active modes of red HgI_2 are[21]

$$\Gamma_R = 3E_g + A_{1g} + 2B_{1g} .$$

Their normal coordinates are given in Appendix B. We will show the calculated Raman tensors of these modes in Table IV. In this calculation the contribution of interlayer I—I′ bonds to the Raman tensors is neglected for intralayer modes. For the B_{1g}^2 rigid layer mode the Raman tensors arising from two groups of interlayer bonds cancel out. Accordingly we get zero Raman tensor. Although interlayer I—I′ bonds would contribute to the Raman tensor for the out-of-plane mode, we neglect this contribution because it is smaller than the contribution from intralayer bonds.

For red HgI_2, only three strong Raman bands are observed at 18, 29, and 114 cm^{-1} and a weak shoulder band is observed at high frequency side of the A_{1g} band at 114 cm^{-1}. The low-lying Raman band at 18 cm^{-1} was assigned to the E_g^3 rigid layer mode.[21] The Raman bands at 29 and 114 cm^{-1} were attributed to E_g^1 and A_{1g} modes,

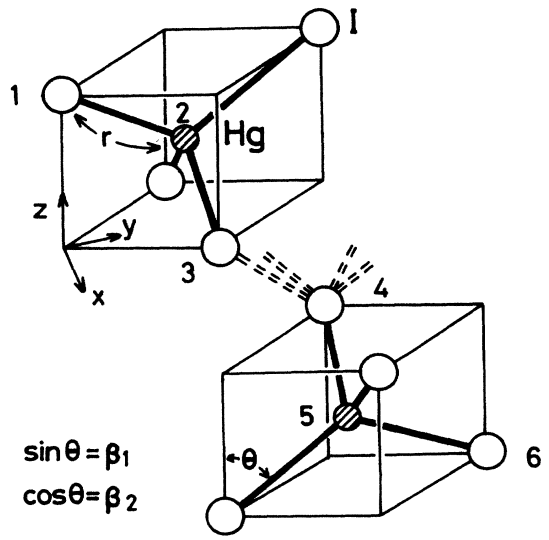

FIG. 3. Structure of red HgI_2. The double broken lines represent interlayer I—I′ bonds.

TABLE IV. The Raman tensors for red HgI_2. The normalization factors in (B1), (B2), (B4), and (B6) are not included in the calculation of the Raman tensors. β_1 and β_2 are a sine and a cosine of the angle between the Hg—I bond and the c axis, respectively.

E_g^1 mode

$$\begin{bmatrix} 0 & 0 & e_1 \\ 0 & 0 & 0 \\ e_1 & 0 & 0 \end{bmatrix}, \quad (x) \qquad \begin{bmatrix} 0 & 0 & 0 \\ 0 & 0 & e_1 \\ 0 & e_1 & 0 \end{bmatrix}, \quad (y)$$

E_g^2 mode

$$\begin{bmatrix} 0 & 0 & e_2 \\ 0 & 0 & 0 \\ e_2 & 0 & 0 \end{bmatrix}, \quad (x) \qquad \begin{bmatrix} 0 & 0 & 0 \\ 0 & 0 & e_2 \\ 0 & e_2 & 0 \end{bmatrix}, \quad (y)$$

$$e_1 = 4\beta_1^2\beta_2(\alpha'_{\parallel} - \alpha'_{\perp}) + \frac{8}{r}\beta_2^3(\alpha_{\parallel} - \alpha_{\perp})$$

$$e_2 = -4(a+b)\beta_1^2\beta_2\left[(\alpha'_{\parallel} - \alpha'_{\perp}) - \frac{2}{r}(\alpha_{\parallel} - \alpha_{\perp})\right]$$

B_{1g}^1 mode

$$\begin{bmatrix} a_1 & 0 & 0 \\ 0 & -a_1 & 0 \\ 0 & 0 & 0 \end{bmatrix} \quad (z)$$

B_{1g}^2 mode

$$\begin{bmatrix} 0 & 0 & 0 \\ 0 & 0 & 0 \\ 0 & 0 & 0 \end{bmatrix} \quad (z)$$

$$a_1 = -4(a+b)\beta_1^2\beta_2\left[(\alpha'_{\parallel} - \alpha'_{\perp}) + \frac{2}{r}(\alpha_{\parallel} - \alpha_{\perp})\right]$$

A_{1g} mode

$$\begin{bmatrix} a_2 & 0 & 0 \\ 0 & a_2 & 0 \\ 0 & 0 & b_2 \end{bmatrix} \quad (z)$$

$$a_2 = 4\beta_1^2\beta_2(\alpha'_{\parallel} - \alpha'_{\perp}) + 8\beta_2\alpha'_{\perp} + \frac{8}{r}\beta_1^2\beta_2(\alpha_{\parallel} - \alpha_{\perp})$$

$$b_2 = 8(\alpha'_{\parallel} - \alpha'_{\perp})\beta_2^3 + 8\beta_2\alpha'_{\perp} - \frac{16}{r}\beta_1^2\beta_2(\alpha_{\parallel} - \alpha_{\perp})$$

respectively. A weak shoulder band at around 145 cm^{-1} was assigned to B_{1g}^1 mode.[22–24] The B_{1g}^2 and E_g^2 modes were missing.

Recently neutron scattering measurements have been made of the low frequency phonon branches.[23] This measurement has revealed that the B_{1g}^2 mode is located at 28.3 cm^{-1} (0.85 THz). This frequency value is very close to that of the E_g^1 mode. From this result Prevot and Biellman[25] have proposed that B_{1g}^2 mode is degenerate with E_g^1 mode and contributes to the Raman intensity of the 29-cm^{-1} band. However, our calculation suggests that the B_{1g}^2 component is very weak compared with the E_g^1 component for this band.

As seen in Table IV, the calculated Raman tensors for the E_g^2 and B_{1g}^2 modes are related to the quantities $\alpha_{\parallel} - \alpha_{\perp}$ and $\alpha'_{\parallel} - \alpha'_{\perp}$. Raman data reported to date have revealed that the E_g^2 mode is missing and the B_{1g}^2 mode is very weak.[14] In view of these results we postulate that $\alpha_{\parallel} \approx \alpha_{\perp}$ and $\alpha'_{\parallel} \approx \alpha'_{\perp}$ in red HgI_2. This hypothesis means that the magnitude of the perpendicular component $\alpha_{\perp}$ relative to $\alpha_{\parallel}$ is large compared with that of IV-IV semiconductors. Lippincott and Stutman attempted to calculate the perpendicular component of the bond polarizability of diatomic molecules.[26] They have suggested that $\alpha_{\perp}$ is obtained from the atomic polarizabilities due to electrons in vicinity of the atoms.

From the considerations it is more likely that the contribution of nonbonded electrons is important for Raman polarizabilities of red HgI_2.

In summary, we have calculated Raman polarizability tensors for typical layered crystals and compared them with the observed spectral profiles. It is suggested that the bond polarizability concept is also applicable to the crystals having ionic character.

The calculated results predict the folded modes of the out-of-plane vibration are missing or very weak except for the $q(0)$ mode, and that the origin of the missing modes is the cancellation of the bond polarizabilities. The comparison with the observation provides information about bonding natures of layered crystals. It is shown that the Raman intensity analysis based on the Raman polarizability is useful to identify observed Raman bands.

ACKNOWLEDGMENTS

The main part of this paper was performed while one of the authors (S.N.) was a visitor at the Université Pierre et Marie Curie. He is grateful to the Ministere de l'Industrie et de la Recherche for financial support.

APPENDIX A

For γ-GaSe which contains a layer in the unit cell, normal coordinates are given by

$$S(E^2)=\begin{cases}a(x_1+x_4)-b(x_2+x_3)\\ a(y_1+y_4)-b(y_2+y_3)\end{cases}, \tag{A1}$$

$$S(E^3)=\begin{cases}a(x_1-x_4)+b(x_2-x_3)\\ a(y_1-y_4)+b(y_2-y_3)\end{cases}, \tag{A2}$$

$$S(E^4)=\begin{cases}a(x_1-x_4)-b(x_2-x_3)\\ a(y_1-y_4)-b(y_2-y_3)\end{cases}, \tag{A3}$$

$$S(A_1^2)=a(z_1+z_4)-b(z_2+z_3)\,, \tag{A4}$$

$$S(A_1^3)=a(z_1-z_4)+b(z_2-z_3)\,, \tag{A5}$$

$$S(A_1^4)=a(z_1-z_4)-b(z_2-z_3)\,. \tag{A6}$$

The coefficients a and b are determined by solving eigenvalue equations for the lattice vibration.

APPENDIX B

The normal coordinates for red HgI_2 are given by

$$S(E_g^1)=\begin{cases}\frac{1}{2}[(x_1-x_3)+(x_4-x_6)]\\ \frac{1}{2}[(y_1-y_3)+(y_4-y_6)]\end{cases}, \tag{B1}$$

$$S(E_g^2)=\begin{cases}(ax_1-bx_2+ax_3)-(ax_4-bx_5+ax_6)\\ (ay_1-by_2+ay_3)-(ay_4-by_5+ay_6)\end{cases}, \tag{B2}$$

$$S(E_g^3,\ \text{RL mode})=\begin{cases}\frac{1}{\sqrt{6}}[(x_1+x_2+x_3)-(x_4+x_5+x_6)]\\ \frac{1}{\sqrt{6}}[(y_1+y_2+y_3)-(y_4+y_5+y_6)]\end{cases}, \tag{B3}$$

$$S(A_{1g})=\tfrac{1}{2}[(z_1-z_3)+(z_4-z_6)]\,, \tag{B4}$$

$$S(B_{1g}^1)=(az_1-bz_2+az_3)-(az_4-bz_5+az_6)\,, \tag{B5}$$

$$S(B_{1g}^2,\ \text{RL mode})=\frac{1}{\sqrt{6}}[(z_1+z_2+z_3)-(z_4+z_5+z_6)]\,. \tag{B6}$$

The coefficients a and b are determined by solving eigenvalue equations for the lattice vibrations.

[1]D. A. Long, Proc. R. Soc. London, Ser. A **217**, 203 (1953).

[2]D. A. Long and A. G. Thomas, Proc. R. Soc. London, Ser. A **223**, 130 (1954).

[3]G. W. Chantry, *The Raman Effect,* edited by A. Anderson (Dekker, New York, 1971), Vol. 1, p. 49.

[4]R. Tubino and L. Piseri, Phys. Rev. B **11**, 5145 (1975).

[5]S. Go, H. Bilz, and M. Cardona, Phys. Rev. Lett. **34**, 580 (1975).

[6]S. Go, H. Bilz, and M. Cardona, in *Proceedings of the Third International Conference on Light Scattering in Solids, Campinas, 1975,* edited by M. Balkanski, R. C. C. Leite, and S. P. S. Porto (Wiley, New York, 1975), p. 377.

[7]A. A. Maradudin and E. Burstein, Phys. Rev. **164**, 1081 (1981).

[8]L. R. Swanson and A. A. Maradudin, Solid State Commun. **8**, 859 (1970).

[9]E. Lopez-Cruz and M. Cardona, Solid State Commun. **45**, 787 (1983).

[10]M. Wolkenstein, C.R. Acad. Sci. URSS, **32**, 185 (1941).

[11]M. Eliashevich and M. Wolkenstein, J. Phys. SSSR **9**, 101 (1945).

[12]S. Nakashima, H. Katahama, Y. Nakakura, A. Mitsuishi, and B. Palosz, Phys. Rev. B **31**, 6531 (1985).

[13]S. Nakashima, H. Katahama, Y. Nakakura, and A. Mitsuishi, Phys. Rev. B **33**, 5721 (1986).

[14]S. Nakashima, M. Hangyo, and A. Mitsuishi, *Vibrational Spectroscopy and Structure,* edited by James R. Durig (Elsevier, Amsterdam, 1985), Vol. 14, p. 305, and references therein.

[15]W. M. Sears, M. L. Klein and J. A. Morrison, Phys. Rev. B **19**, 2305 (1979).

[16]S. Nakashima, H. Katahama, and A. Mitsuishi, Physica **105B**, 343 (1981).

[17]See for example, T. J. Wieting and J. L. Verble, *Electrons and Phonons in Layered Crystal Structures,* edited by T. J. Wieting and M. Schlüter (Reidel, Dordrecht, 1979), p. 321, and references therein.

[18]R. M. Hoff, J. C. Irwin and R. M. A. Lieth, Can. J. Phys. **53**, 1606 (1975).

[19]A. Polian, K. Kunc, and A. Kuhn, Solid State Commun. **19**, 1079 (1976).

[20]For a recent review, see C. Y. Fong and M. Schlüter, in *Electrons and Phonons in Layered Crystal Structures,* edited by T. J. Wieting and M. Schlüter (Reidel, Dordrecht, 1979), p. 145.

[21]S. Nakashima, H. Mishima, and A. Mitsuishi, J. Raman Spectrosc. **1**, 325 (1973).

[22]Y. Ogawa, I. Harada, H. Matsuura, and T. Shimanouchi, Spectroschim. Acta **32a**, 49 (1976).

[23]B. Prevot, C. Schwab, and B. Dorner, Phys. Status Solidi B **88**, 327 (1978).

[24]V. A. Haisler, V. M. Zaletin, A. F. Kravchenko, and G. Y. Yashin, Phys. Status Solidi B **121**, K13 (1984).

[25]B. Prevot and J. Biellmann, Phys. Status Solidi B **95**, 601 (1979).

[26]E. R. Lippincott and J. M. Stutman, J. Phys. Chem. **68**, 2926 (1964).